



# Numerical study of crack path by MMCG specimen using M integral

S. El Kabir, R. Moutou Pitti

Université Clermont Auvergne, Université Blaise Pascal, Institut Pascal, PB 10448, 63000, Clermont-Ferrand, France

CNRS, UMR 6602, Institut Pascal, 63171, Aubière, France

*soliman.elkabir@yahoo.fr, rostand.moutou\_pitti@univ-bpclermont.fr*

N. Recho

Université Clermont Auvergne, Université Blaise Pascal, Institut Pascal, PB 10448, 63000, Clermont-Ferrand, France

CNRS, UMR 6602, Institut Pascal, 63171, Aubière, France

*recho@moniut.univ-bpclermont.fr*

and EPF Ecole d'ingénieurs, Sceaux, France

*naman.recho@epf.fr*

Y. Lapusta

French Institute of Advanced Mechanics, Université Clermont Auvergne, Institut Pascal UMR 6602 / UBP / CNRS / IFMA, PB 265, 63175, Aubière, France

*lapusta@ifma.fr*

F. Dubois

GEMH Laboratory, Limoges University, Civil Engineering Center, 19300, Egletons, France

*Frederic.dubois@unilim.fr*

**ABSTRACT.** The mixed mode loading configuration occurs in many civil engineering and mechanical applications. In wood material, the study of this problem is very important due to the orthotropic character and the heterogeneity of the material. In order to study the mixed mode loading in wood material, Moutou Pitti et al [1] have proposed a new specimen called Mixed Mode Crack Growth (MMCG). The main goal of this geometry is to propose a decrease of the energy release rate during the crack growth process. In this case, the fracture parameters can be decoupled into Mode I and Mode II in order to determine the impact of time during creep crack test. The present work proposes to study the crack path stability in MMCG specimen for different sizes and thicknesses. The  $M\theta$  integral, combining real and virtual mechanical displacement fields is used in order to separate numerically mode I and mode II in the mixed mode ratio. The stability is shown for the opening mode (Mode I), the shear mode (Mode II), and the mixed mode of  $15^\circ, 30^\circ, 45^\circ, 60^\circ, 75^\circ$  by computing the energy release rate versus the crack length. Finally, it is shown that the MMCG specimen can be reduced in various shape and used for example in small climate chamber in order to perform creep test at different temperature and moisture content levels.

**KEYWORDS.** Crack stability; MMCG specimen; M integral; Energy release rate.

## INTRODUCTION

Civil engineering and mechanical structures are usually submitted to mixed mode loading. As a consequence, a mixed mode crack growth process occurs. This fact appears again as an important key in the case of wood material due to its orthotropic behavior and heterogeneous character of the material. Also, in order to know the real impact of time effects on the damage process during creep crack growth tests, it is necessary to separate fracture effects and time effect. In this case, Moutou Pitti & al [1] have proposed new specimen for mixed mode fracture of wood called Mixed Mode Crack Growth (MMCG), Fig. 1 (c). This specimen is a combination of a modified Double Cantilever Beam (DCB) developed by Dubois, but just usable in opening mode [2], Fig. 1 (a), and a Cantilever Tension Shear (CTS) specimen developed by Richard [3,4] and used by Ma and Zhang for metallic material [5] and adapted by Valentin and Caumes for timber material [3], Fig. 1 (b).

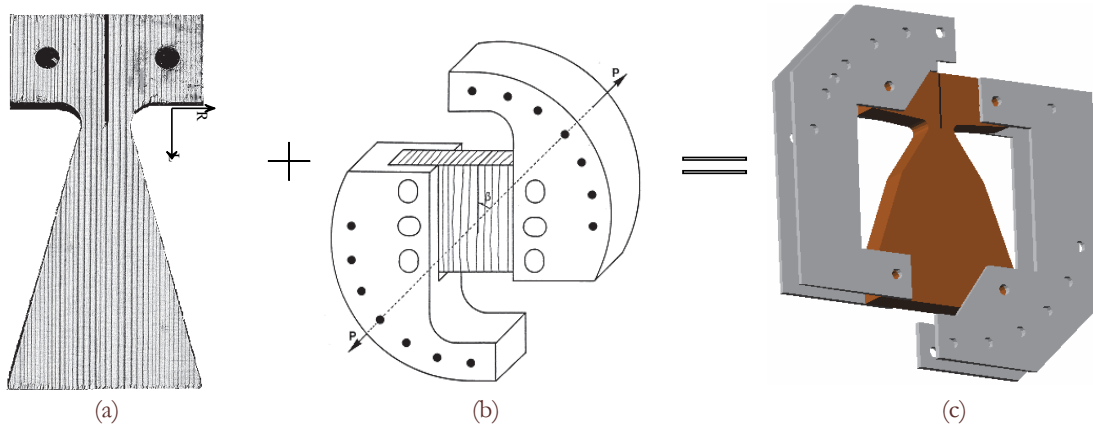


Figure 1: (a) Modified Double Cantilever Beam DCB specimen [2]. (b) Cantilever Tension Shear CTS specimen [6]. (c) Mixed mode Crack Growth MMCG specimen [1].

Although, according to its large sizes, the MMCG specimen developed by Moutou Pitti & al [1] is not adapted to all humidity and temperature test chambers. It is necessary to have specimens with various dimensions to realize experiment tests in different configurations, in order to evaluate fracture parameters, and to study thermo-mechanics and mechano-sorptive effects [2]. Based on the previous specimen [1], we propose to study three different size ratios and three thickness ratios  $\frac{3}{4}$ ,  $\frac{1}{2}$ ,  $\frac{1}{4}$ , according to the initial MMCG geometry. For each case we plot the evolution of the energy release rate versus the crack length. The numerical analyses of crack path under mixed mode loading are performed as function of contour integral. The  $M\Theta$  integral allows determining the crack growth behavior under mixed mode ratio. The computation is realized for an orthotropic elastic material assuming a plane stress state.

In the present work, in order to determine the crack stability in the opening mode, shear mode and mixed mode, we analyze several new sizes and thicknesses of the MMCG specimen. The first section recalls some integral parameters that we use in calculating the energy release rate around the crack tip. The second part presents a MMCG specimen as proposed by Moutou Pitti e & al [1], including its design and geometry and some results under mixed mode for  $45^\circ$ . The last section introduces some new dimensions of a MMCG specimen under different loadings and gives for each case the evolution of the energy release rate versus the crack length. Crack growth stability in mixed mode is justified by the decrease of the energy release rate along the crack path.

## INTEGRAL PARAMETER

In this section we present the path integral which enabled us to obtain the energy release rate  $G$  under mixed mode solicitation. A path independent integral is equivalent to the energy release rate. For cracked linear elastic material, Rice [7] have used J-integral to compute energy release rate for curvilinear contour. J-integral takes the following notation:

$$J = \int_{\Gamma_1} \left( F \cdot n_1 - \sigma_j n_j \frac{\partial u_i}{\partial a} \right) \cdot n_j d\Gamma_1 = G \quad (1)$$



Where  $\Gamma_1$  is arbitrary curvilinear contour oriented by its normal vector  $\vec{n}$ ,  $F$  denotes the Helmholtz strain energy density,  $u_i$  is the displacement component and  $\sigma_{ij}$  is the stress component.

### M and $M\theta$ integral

M-integral is an energetic approach that allows studying stress field around crack tip. It is developed by Chen and Shield [8] in order to separate mixed mode fracture [8] and is a combination between real and virtual strain fields which enables computing fracture parameter. Based on a conservative law, M-integral enables to separate fracture mode under creep mixed load [9]:

$$M = \frac{1}{2} \int_{\Gamma} (\sigma_{ij}^r \cdot u_j - \sigma_{ij}^u \cdot v_{i,1}) \cdot n_j d\Gamma \quad (2)$$

Where  $\sigma_{ij}$  and  $\sigma_{ij,1}^r$  are real and virtual stresses associated with the real and virtual displacements fields  $u$  and  $v$ . The curvilinear integral (2) is difficult to realize in the finite element method [1, 2, 9]. In order to make easy numerical integration Destuynder [10] proposed  $M\theta$  integral. This integral is obtained by Ostrogradski transformation and defined at a surface contour containing the crack tip.

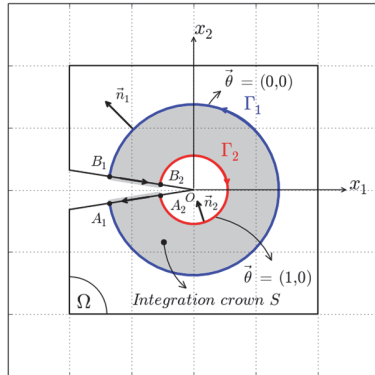


Figure 2: Integral domain of  $M\theta$ .

$$M\theta = \frac{1}{2} \int_V (\sigma_{ij}^u \cdot v_{i,k} - \sigma_{ij,k}^r \cdot u_i) \cdot \theta_{k,j} dV \quad (3)$$

where  $\theta$  is a continuous and derivable scalar field. It forms a crown around the crack tip as shown in Fig. 2.

### Energy release rate

In general case the energy release rate, denoted  $G$ , traduces the energy release by the material during an unitary crack growth process. According to this definition, the energy release rate, is the energy consumed by the crack growth  $\Delta a$  [16] and takes the following expression

$$G = \frac{\partial W_{pot}}{\partial a} \quad (4)$$

$dW_{pot}$  is the variation of the potential energy. In simple mode solicitation, the energy release rate can be defined by Eq. (1) or Eq. (4). However, in mixed mode loading, using the superposition principle one can write the following relation [11]:

$$M\theta(u, v) = C_1 \frac{K_I^u \cdot K_I^v}{8} + C_2 \frac{K_{II}^u \cdot K_{II}^v}{8} \quad (5)$$

$C_1$  and  $C_2$  are the reduced elastic compliances and  $K_I$  and  $K_II$  are the stress intensity factors in opening mode and shear mode, respectively. In order to decouple each fracture mode and obtain the real stress intensity factors  $K_I''$  and  $K_{II}''$ , we perform two computations of particular values of virtual stress intensity factors  $K_I^v$  and  $K_{II}^v$  [1] as follows

$$K_I'' = 8 \frac{M\theta(K_I^v = 1, K_{II}^v = 0)}{C_1} \text{ and } K_{II}'' = 8 \frac{M\theta(K_I^v = 0, K_{II}^v = 1)}{C_2} \quad (6)$$

Finally, we can compute the energy release rate for each mode by combining expressions (4) and (5) according to real intensity factors:

$$G = G_I + G_{II} = C_1 \cdot \frac{(K_I'')^2}{8} + C_2 \cdot \frac{(K_{II}'')^2}{8} \quad (7)$$

## MMCG SPECIMEN

### Design and geometry

**A**s described in introduction, the Mixed Mode Crack Growth (MMCG) specimen is a combination between modified DCB and CTS [1]. In this part, we recall the wood specimen dimensions of MMCG device. Fig. 3 presents the dimensions in millimeters of the initial wood specimen proposed in [1]. In this wood specimen, four holes are machined in order to fixe the Arcan device. This allows a various mixed ratio with seven loading fixations with angle  $\theta = (0^\circ ; 15^\circ ; 30^\circ ; 45^\circ ; 60^\circ ; 75^\circ ; 90^\circ)$ . The geometry of the MMCG specimen has been optimized by using a finite element computation. The main goal of this specimen is to obtain a stable crack growth rate during propagation.

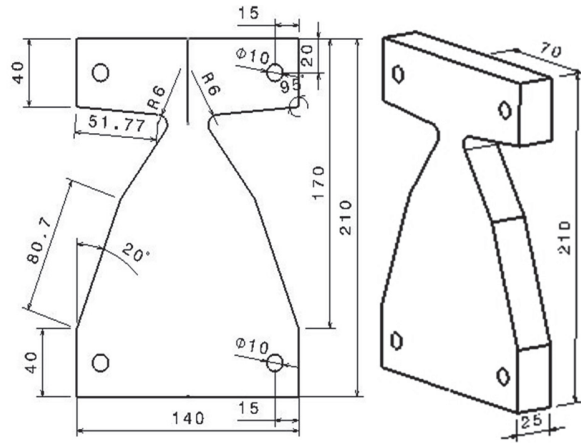


Figure 3: MMCG specimen.

The finite element computation is realized in plane stress state for an elastic orthotropic behavior. Wood material used is Douglas fir and has the following elastic characteristics: longitudinal modulus  $E_x=14100 \text{ MPa}$ , transversal modulus  $E_y=2040 \text{ MPa}$ , shear modulus  $G_{xy}=925 \text{ MPa}$ , Poisson ratio  $\nu_{xy}=0.4$ .

### Crack growth stability

MMCG specimen was designed in order to obtain the crack growth stability. The decrease of the energy release rate translates stability of the crack growth. In mixed mode loading and according to the Griffith approach, Moutou Pitti et al. have introduced a threshold function [1] such as:

$$f = \frac{G_1}{G_1'} + k \frac{G_2}{G_2'} \quad (8)$$



$G_1^*$  and  $G_2^*$  are the critical values of the energy release rate in each mode respectively. They are parameters depend your material characteristics. The factor  $k$  is the mixed mode ratio equal to 1 in the present work. According to equation (7), the crack growth process obeys to the three different cases:

- Crack growth initiation  $f < 1$
- Crack growth stability  $f = 1$  and  $\frac{\partial f}{\partial a} < 0$
- Crack growth instability  $f > 1$  and  $\frac{\partial f}{\partial a} > 0$

where  $a$  is the crack length.

## NEW SPECIMEN DIMENSIONS AND CRACK GROWTH STABILITY

### Design and geometry

In order to prove the efficiency of new specimen, various size and thickness parameters of MMCG are presented in Fig. 4 for mixed loading mode at  $45^\circ$ .

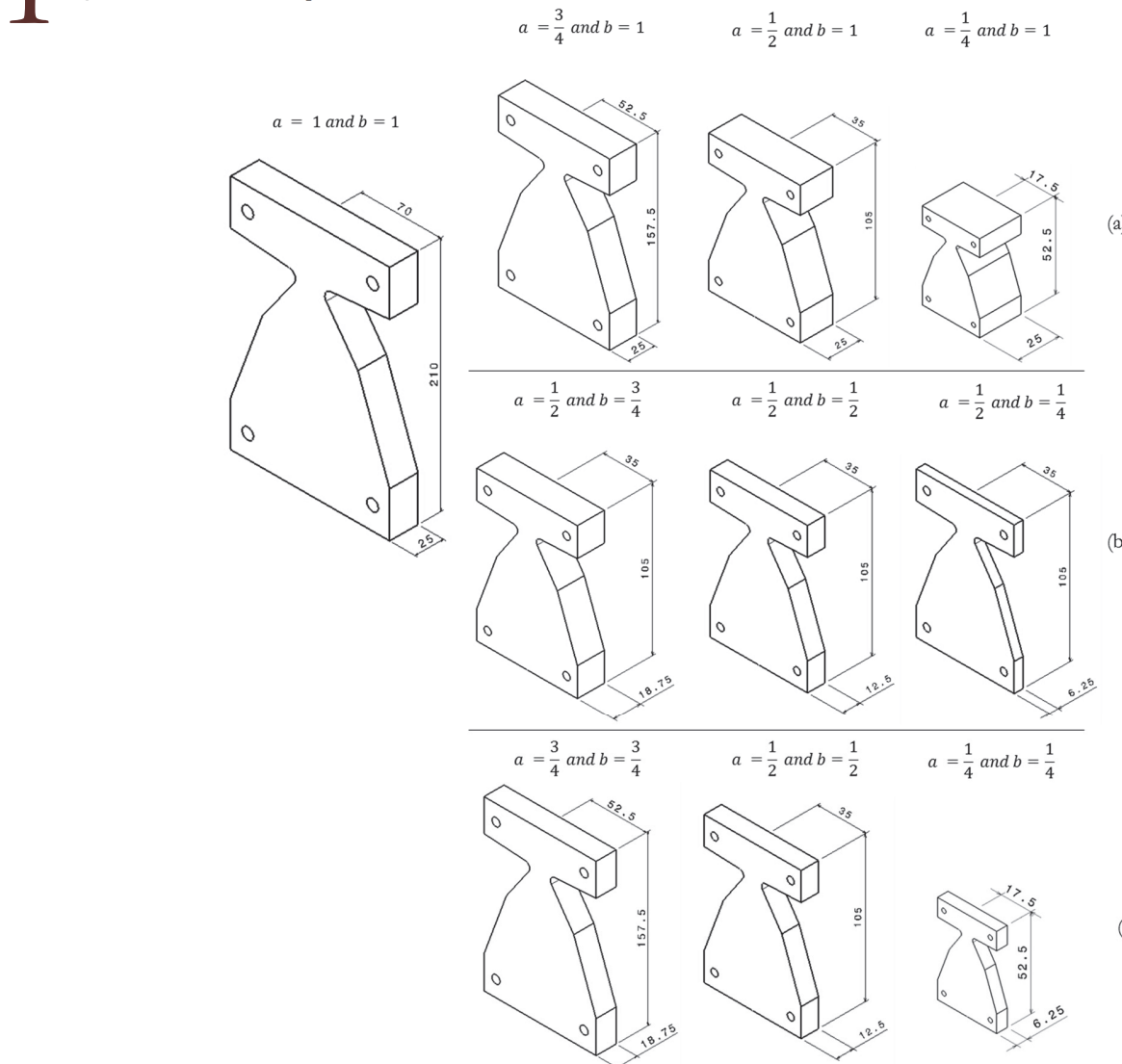


Figure 4: Geometric definition of MMCG specimen for: (a): different size coefficients  $a$ , (b): different thicknesses coefficients  $b$  and (c): a combination of both.

The initial crack length is fixed to  $49 \text{ mm} * a$ , with the coefficient  $a = 1; \frac{3}{4}; \frac{1}{2}; \frac{1}{4}$ . The factor  $b$  is used to modify the thickness and takes the following values  $b = 1; \frac{3}{4}; \frac{1}{2}$ . For different MMCG specimens, the simulation presents a crack growth process to a final crack length of 70 iterations.

In the literature, the initial Arcan fixture is proposed by [1]. In this work, new shapes and dimensions of the experimental loading device are proposed, see e.g. Fig. 5. The system allows considering, during the test, the specimens for the factor  $a = \frac{1}{2}$  and  $a = 1$ , and different thicknesses for MMCG specimen.

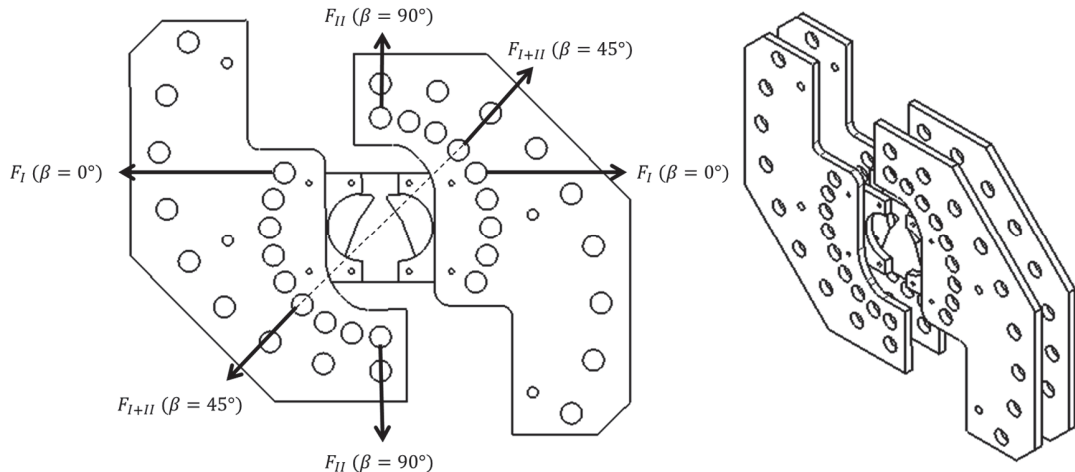


Figure 5: MMCG specimen and loading device adapted for  $a = 1$  and  $a = \frac{1}{2}$ .

### Numerical results

In this section, the results of parametrical study are exposed. In order to observe the stability of MMCG specimen, the energy release rate is computed for different sizes and thicknesses of the MMCG specimen. Finite element computation is realized with the software Cast3m, produced by French Energy Atomic Commission CEA [12]. For some significant cases, we plot the evolution of the energy release rate as function of the crack growth. The decrease of the energy release rate for specimen of new sizes translates the stability of the crack growth. The computation is realized assuming a plane stress state. Radial meshes and  $\theta$  field are shown in Fig. 6. In Fig 6 (a), the size of radial mesh and the field  $\theta$  are the same, and the mesh is constructed with 10 elements around the crack tip. Greater is the number of elements, more accurate is  $M\theta$  value. For more stability,  $M\theta$  field has to be included inside the radiating mesh as seen in Fig 6 (b). Mesh density and  $M\theta$  field are two parameters which allow less disruption and more numerical stability.

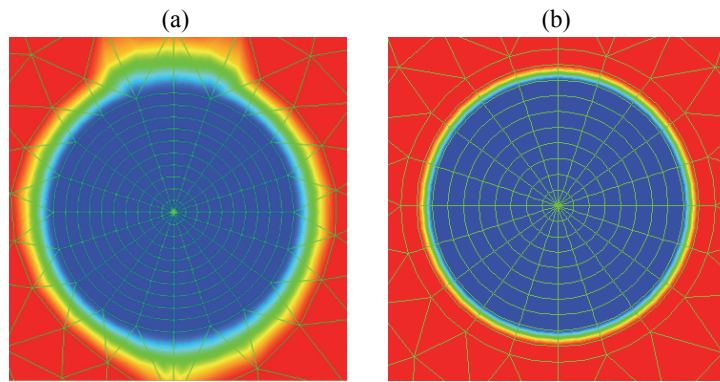


Figure 6:  $M\theta$  field around the crack tip and outside radial meshes (a), or inside radial meshes (b).

Fig. 7 presents the contributions of the opening mode and the shear mode to the energy release rate for the mixed mode ratio of  $45^\circ$  for different size coefficients  $a$  and the same thickness. In Fig. 7 (a), results for three different sizes versus crack length are presented and we show that the value of  $G$  increases when the size increases. Simultaneously, Fig. 7 (b) and (c)



show stable crack growth zones for 2 sizes. The results are summarized in Table 1 where different new size parameters are given versus stable crack growth zones.

Fig. 8 (a) illustrates the evolution of the energy release rate versus the crack length for several MMCG specimen thicknesses  $b$  and size  $a=1$ .  $G_1$  and  $G_2$  are the parts of opening and shear in the mixed mode 45°. We observe that the values of  $G$  increase when the thickness decreases. Stable crack growth zones are also presented in Fig. 8 (b) and (c).

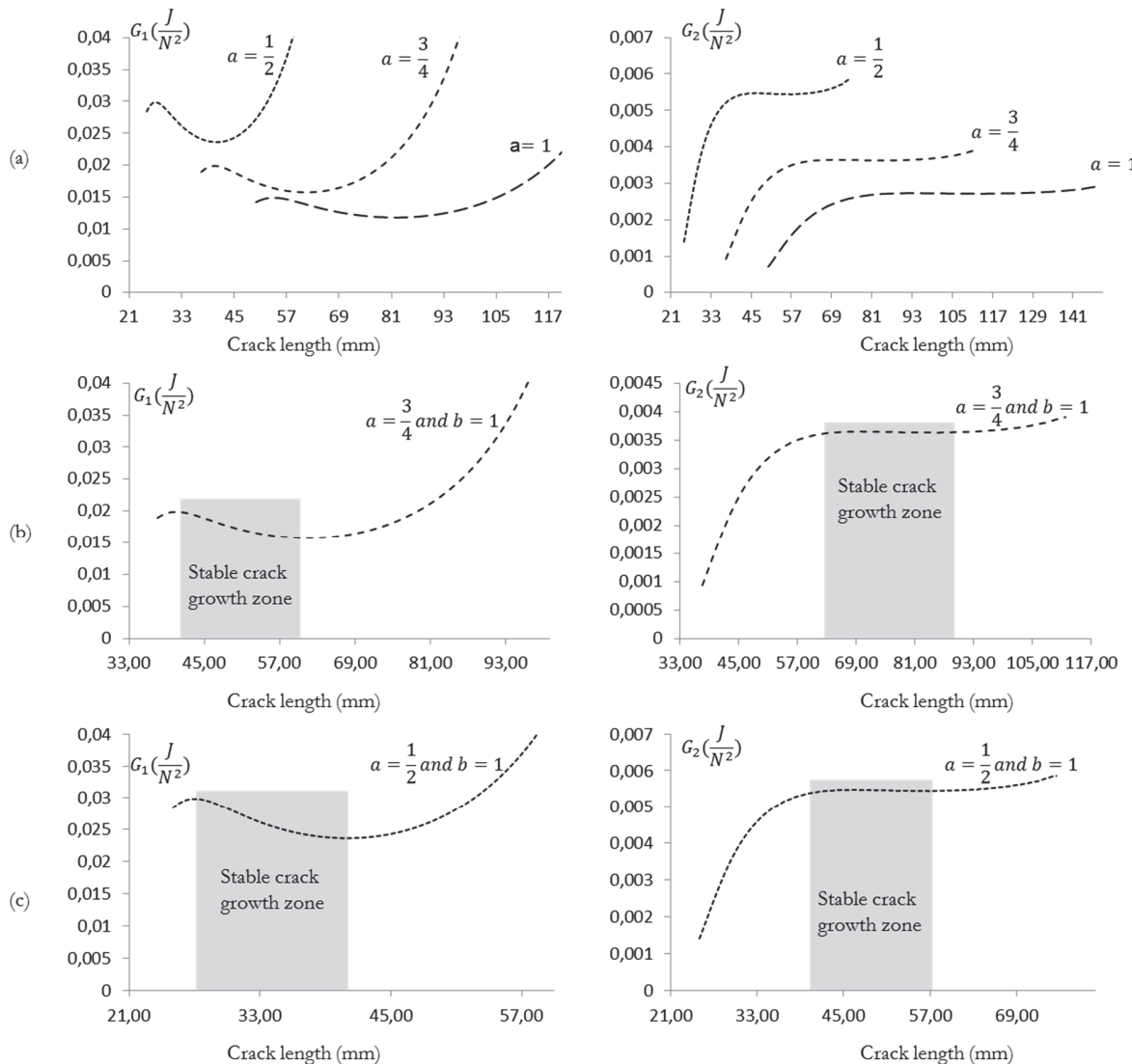


Figure 7: Normalized elastic energy release rate  $G_1$  and  $G_2$  versus mixed mode ratio for various sizes parameter  $a = \left\{ 1; \frac{3}{4}; \frac{1}{2} \right\}$  and  $b = 1$  (a), for  $a = \frac{3}{4}$  and  $b = 1$  (b), for  $a = \frac{1}{2}$  and  $b = 1$  (c).

Size parameter a	Stable zone $G_1$ (mm)	Length of stable zone $G_1$ (mm)	Stable zone $G_2$ (mm)	Length of stable zone $G_2$ (mm)
1	[54:82]	28	[93:114]	21
0.75	[40.5:61.5]	21	[69.75:85.5]	15.75
0.5	[27:41]	14	[46.5:57]	10.5
0.25	[13.5:20.5]	7	[23.25:28.5]	5.25

Table 1: Stable crack growth zones for different size parameter and  $b = 1$ .

Tab. 1 shows the stable crack growth zones for various new size parameters. The lengths are proportional to size parameter and greater for  $G_1$  than for  $G_2$ .

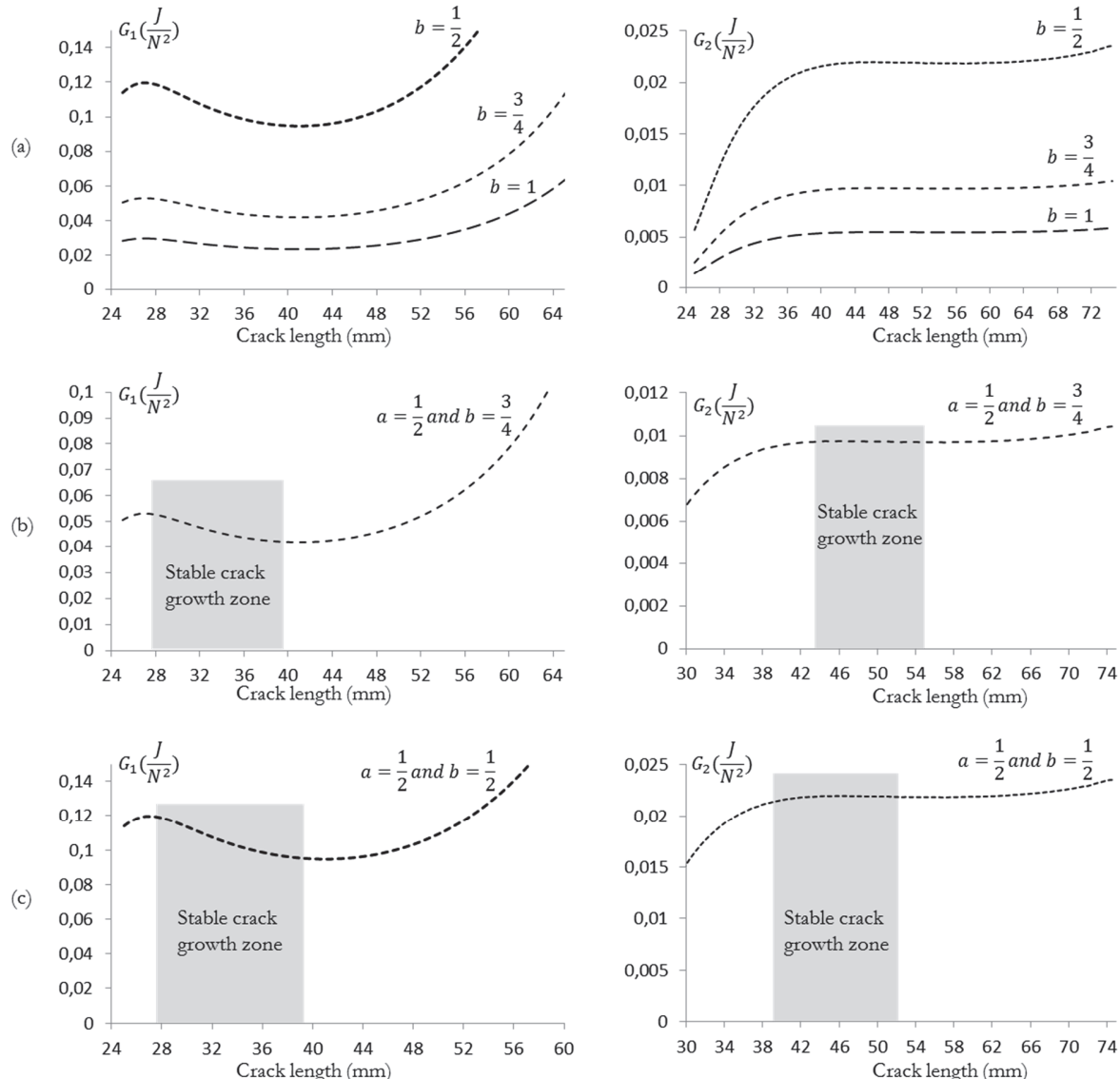


Figure 8: Normalized elastic energy release rate  $G_1$  and  $G_2$  versus mixed mode ratio for various thickness parameters  $b = \left\{1; \frac{3}{4}; \frac{1}{2}\right\}$  and  $a = \frac{1}{2}$  (a), for  $a = \frac{1}{2}$  and  $b = \frac{3}{4}$  (b), for  $a = \frac{1}{2}$  and  $b = \frac{1}{2}$  (c) .

Comparison between  $G_1$  and  $G_2$  shows that the opening mode needs 10 times more energy than the shear mode.

Thickness parameter b	Stable zone $G_1$ (mm)	Stable zone $G_2$ (mm)
1	[27:41]	[46.5:57]
0.75	[27:41]	[46.5:57]
0.5	[27:41]	[46.5:57]
0.25	[27:41]	[46.5:57]

Table 2: Stable crack growth zone for different size parameter and  $a = \frac{1}{2}$ .



Tab. 2 shows the stable crack growth zones for various new thickness parameters. The length of stable zones is the same for all cases.

Let us analyze now the influence of the thickness on the energy release rate. As shown in Fig. 9, a thickness change results in a new value of the energy release rate.

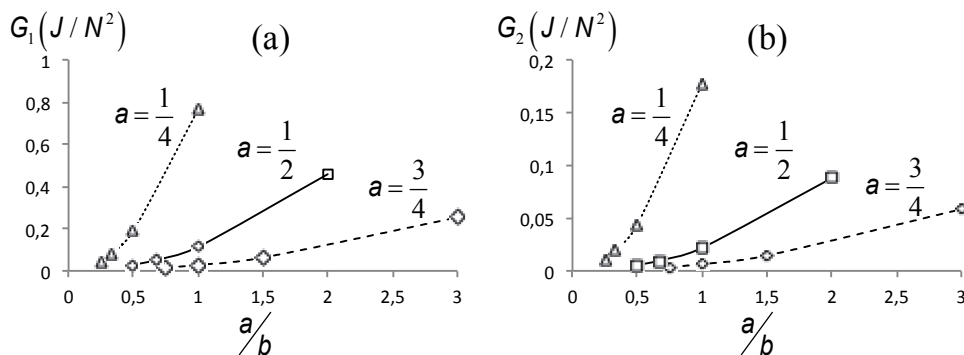


Figure 9: Influence of  $a/b$  ratio on the energy release rate evolution

The evolution of the energy release rate are not linearly dependent on the  $a/b$  ratio, see Fig. 9. The change of thickness has an impact on the MMCG specimen. We consider, in numerical computation by integral under the plane stress assumption, that the effort is divided by thickness.

Dependencies of  $G_1$  and  $G_2$  versus  $a/b$  ratio are posted in Fig. 9 (a) and (b) respectively. We show the influence of the thickness parameter  $b$  on the MMCG specimen stability for various cases of the size parameter  $a$ .

## CONCLUSION AND FUTURE EXTENSIONS

In this work, different sizes and thicknesses of Mixed Mode Crack Growth (MMCG) specimen have been studied numerically. The evolution of the energy release rate versus the crack length for each new size and thickness of a new MMCG specimen have been determined. Numerical calculations have been performed for the ratio of mixed mode 45°. The stability is justified by the decrease of  $G$  versus crack length during the growth process in each mode. This parametric study shows the impact of size, thickness, and both parameters combined on the energy release rate coupled with the crack stability. The following conclusions can be drawn:

- The MMCG specimen is stable for the parameters studied;
- The smaller are the dimensions of the MMCG specimen, the more the stability is reduced;
- The variation in thickness impacts the evolution of the energy release rate  $G$ .

In future work, it will be necessary to extend the numerical computation to a pure opening mode, pure shear mode, and different angles in mixed mode in order to optimize MMCG specimen for larger stability zone. Also, experimental tests will be necessary to validate the numerical results. This study can be extended to perform new crack extension criteria under mixed mode loading [13, 14] for composite materials [15].

## REFERENCES

- [1] Moutou Pitti, R., Dubois, F., Pop, O., A proposed mixed-mode fracture specimen for wood under creep load, *Int. J. Fract.*, 167(2011) 195–209.
- [2] Dubois, F., Chazal, C., Petit, C., Viscoelastic crack growth process in wood timbers: An approach by the finite element method for mode I fracture, *Int. J. Fract.*, 113(4) (2002) 367-388.
- [3] Richard, H., Benitz, K., A loading device for the creation of mixed mode in fracture mechanics, *Int. J. Fract.*, 22 (1983) 55-58.
- [4] Richard, H., A new compact shear specimen *Int. J. Fract.*, 17 (1981) 105-107
- [5] Ma, S., Zhang, X., Recho, N., Li, J., The mixed-mode investigation of the fatigue crack in CTS metallic specimen, *Int. J. Fatig.*, 28 (2006) 1780–1790.



- [6] Valentin, G., Caumes, P., Crack propagation in mixed mode in wood: a new specimen, *Wood Science and Technology*, 23 (1989) 43-53.
- [7] Rice, J.R., A path independent integral and the approximate analysis of strain concentrations by notches and cracks, *J. Appl. Mech.*, 35 (1968) 379–386.
- [8] Chen F.M.K., Shield, R.T., Conservation laws in elasticity of J-integral type, *J. Appl. Mech. Phys.*, 28 (1977) 1–22.
- [9] Moutou Pitti, R., Dubois, F., Petit, C., Sauvat, N., Pop, O., A new M-integral parameter for mixed-mode crack growth in orthotropic viscoelastic material, *Eng. Fract. Mech.*, 75 (2008) 4450–4465.
- [10] Destuynder, Ph., Djaoua, M., Lescure, S., Quelques remarques sur la mécanique de la rupture élastique, *J. de Mécanique Théorique et Appliquée*, 2 (1983) 113–135.
- [11] Moutou Pitti, R., Dubois, F., Petit, C., Sauvat, N., Mixed mode fracture separation in viscoelastic orthotropic media: numerical and analytical approach by the M $\theta$ v-integral, *Int. J. Fract.*, 145 (2007) 181–193. doi:10.1007/s10704-007-9111-4.
- [12] CEA Commissariat de l'Energie Atomique, <http://www-cast3m.cea.fr/index.php?xml=download1>, France (2014).
- [13] Li, J., Zhang, X. B., Recho, N., J-Mp based criteria for bifurcation assessment of a crack in elastic-plastic materials under mixed mode I-II loading, *Eng. Fract. Mechanics*, 71 (2004) 329-343.
- [14] Zhang, X., Ma, S., Recho, N., Li, J., Bifurcation and propagation of a mixed-mode crack in a ductile material, (2006) 1925–1939.
- [15] Lapusta, Y., Henaff-Gardin C., An analytical model for periodic alpha-layer cracking in composite laminates, *International Journal of Fracture*, 102 (2000) 73-76.
- [16] Griffith, A. A., The phenomena of rupture and flow in solids, *Philosophical Transactions of the Royal Society*, 221 (1921) 163-198.